WCAP-16996-P, "Realistic LOCA Evaluation Methodology Applied to the Full Spectrum of Break Sizes (FULL SPECTRUM LOCA Methodology)"
Request for Additional Information – (Non-Proprietary)
RAIs 77-82, 86-87, 93 and 112

March 2014

Westinghouse Electric Company LLC
1000 Westinghouse Drive
Cranberry Township, PA 16066

Question #77 (RAI Set 6): Loop Seal Clearance in LSTF Test SB-CL-18

WCAP-16996-P/WCAP-16996-NP, Volumes I, II and III, Revision 0, Section 18, "Loop Seal Clearance," Subsection 18.2, "Important Physical Processes and Scaling Laws, " Subsection 18.2.1, "ROSA," considers experimental data from two integral effects, Test SB-CL-18 and Test SB-CL-14, performed at the LSTF as part of the ROSA No. 4 (ROSA-IV) test program. LSTF was a full-pressure facility and preserved major component elevations of the reference Westinghouse-type four-loop 3,423 MWt (1,110 MWe) PWR at Tsuruga Unit 2 of Japan Atomic Power Company. The LSTF had an overall volumetric scaling ratio of 1/48 and featured two equal-volume primary loops. The hot and cold legs had an ID of 0.207 m (8.15 inch) determined to preserve the loop volumetric scaling ratio 2/48 and the length to square-root-of-diameter ratio ($L/\sqrt{D}$) for flow regime simulation. The prototypical PWR hot and cold leg IDs were 0.7366 m (29 inch) and 0.6985 m (27.5 inch), respectively. The cross-over legs of the loop seals in LSTF had an ID of 0.1682 m (6.62 in), compared to a prototypical cross-over leg diameter of 0.7874 m (31 inch), to scale volume and preserve height. In Test SB-CL-18 and Test SB-CL-14, the break unit was connected horizontally to the cold leg between the RCP and the RPV in Loop B, which was not connected to the pressurizer.

Test SB-CL-18 simulated a 5 percent cold leg break, which corresponds to a break area of 0.205 ft^2 or a 6.1 inch equivalent break diameter based on the reference PWR cold leg diameter (27.5 inch). Test data is documented by H. Kumamaru et al., "ROSA-IV/LSTF Cold Leg Break LOCA Experiment Run SB-CL-18 Data Report," Japan Atomic Energy Research Institute Report JAERI-M 89-027, March 1989. Loop seal clearing occurred in both loops at approximately 140 s after the break. Core uncovery took place temporarily between approximately 120 s and 155 s during loop seal clearing and most of the core heater rods experienced superheating of up to about 342 °F (190 K). PCT of approximately 872 °F (740 K) was observed during the core uncovery just prior to loop seal clearing.

Figure A.2, "Primary Loop A Instruments (II)," in JAERI-M 89-027 shows the instrumentation in the intact loop and Figure A.4, "Primary loop B Instruments (II)," in the same report shows the instrumentation in the broken loop. JAERI-M 89-027, Figure 5.32, "Differential Pressure LSA, PCA," plots measurements from differential pressure transducer DPE070 in the loop seal downhill side (channel DPE070-LSA, DP 17) and from transducer DPE080 in the loop seal uphill side (data channel DPE080-LSA, DP 19). Figure 5.33, "Differential Pressure LSB, PCB," exhibits measurements from transducer DPE210 in the loop seal downhill side (channel DPE210-LSB, DP 41) and from transducer DPE220 in the loop seal uphill side (data channel DPE220-LSB, DP 42). As reflected by the DPE210 data in Figure 5.33, the liquid level in the descending loop seal section, connected to the SG exit chamber, reduces significantly from an initial quasi steady-state absolute value of about 43 kPa (6.3 psid) down to an absolute value of about 8 kPa (1.2 psid) at approximately 140 s after the break. At this point, loop seal clearance begins as seen from DPE220 signal for the ascending loop seal section. The process occurs during a time window of about 60 s and it is completed by 200 s after the break. During loop seal clearance, the DPE220 signal in the ascending loop seal section reduces sharply from an initial quasi steady-state value of about 24 kPa (3.5 psid) to approximately 2 kPa (0.3 psid) whereas the DPE210 signal in the descending loop seal section decreases further only slightly from 8 kPa to about 6 kPa (0.9 psid). The data measurements for the intact loop seal shown in Figure 5.32 exhibit a similar behavior.

Subsection 18.2.1 of the TR WCAP-16996-P/WCAP-16996-NP, Volumes I, II, and III, Revision 0, presents a single plot of Test SB-CL-18 data in Figure 18.2.1-1a, "Measured Pressure Drop in Broken Loop of ROSA 5 percent Break (Kumamaru, et al., 1989)." Figure 18.2.1-1a is a reproduction of Figure 5.33 in the JAERI-M 89-027 report. Referring to the Test SB-CL-18 data in Figure 18.2.1-1a, it is observed in Subsection 18.2.1 that "the liquid tends to be pushed towards the uphill bend and up the pump suction leg." Subsection 18.2.1 continues by stating that "this suggests that the remaining liquid after loop seal clearing will tend to be collected in the uphill side of the loop seal."

(1) The DPE220 signal in the uphill loop seal section reproduced in Figure 18.2.1-1a, "Measured Pressure Drop in Broken Loop of ROSA 5 percent Break (Kumamaru, et al., 1989)," for Test SB-CL-18 shows only a very small differential pressure of about 2 kPa towards the end of the loop seal clearance phase at 200 s. During the following part of the transient, the measurement reduces gradually down to zero at approximately 650 s and remains at this level thereafter. The DPE210 signal in the descending loop seal section shows a relatively small, in absolute value, differential pressure, which reduces slightly from approximately 6 kPa down to 3.5 kPa during the depicted post-clearance period from 200 s to 900 s. Please clarify how the DPE210 and DPE220 differential pressure measurements shown in Figure 18.2.1-1a support the interpretation in WCAP-16996-P/WCAP-16996-NP, Volumes I, II and III, Revision 0, Subsection 18.2.1 that liquid remaining in the loop seal piping following the loop seal clearance "will tend to be collected in the uphill side of the loop seal."

(2) Based on "assessment of WCOBRA/TRAC-TF2 relative to the experiments indicates," WCAP-16996-P/WCAP-16996-NP, Volumes I, II and III, Revision 0, Subsection 18.4, "Conclusions," states, among other findings, that "the remaining liquid retained after loop seal clearing tends to collect in the uphill bend and RCP suction leg, as demonstrated in the ROSA tests (Section 21)." WCAP-16996- P/WCAP-16996-NP, Volumes I, II and III, Revision 0, Section 21, "ROSA-IV Test Simulations," Subsection 21.4.3, "Results and Conclusions from the SB-CL-18 Simulation," refers to Figures 21.4-1 through 21.4-20 when comparing code predictions against Test SB-CL-18 measurements. Figures 21.4-3 and 21.4-4 show a comparison of the calculated and measured loop seal differential pressures in both loops. It is stated in WCAP-16996-P/WCAP-16996-NP, Volumes I, II and III, Revision 0, Subsection 21.4.3 that [ ][a,c] and clarifies that "the test data and calculations also show that after the loop seals clear, steam venting is established through both crossover legs." Please explain which evidence from Test SB-CL-18, as presented in WCAP-16996-P/WCAP-16996-NP, Volumes I, II and III, Revision 0, Section 21, Subsection 21.4, "Simulation of SB-CL-18, 5-Percent Cold Leg Side," supports the conclusion in Subsection 18.4 that "assessment of WCOBRA/TRAC-TF2 relative to the experiments indicates that "the remaining liquid retained after loop seal clearing tends to collect in the uphill bend and RCP suction leg, as demonstrated in the ROSA tests (Section 21)." Please present any additional experimental measurements and specific analyses, as appropriate, in support of this conclusion.

Response:

The intent of the quoted text is to say that "the remaining liquid retained in the cross-over leg after the onset of the loop seal clearing tends to collect in the uphill bend and RCP suction leg."

As noted in the RAI, the onset (beginning) of the loop seal clearing at the SB-CL-18 test does appear to be around 140 seconds after the break; this is when the differential pressures measured on the descending part of the cross-over leg (DPE070-LSA, Figure 21.4-3 and DPE210-LSB, Figure 21.4-4) are at about 8 kPa. During the following (~60-sec) loop seal clearing time window, the differential pressures measured on the ascending sides (DPE080-LSA and DPE220-LSB) gradually decrease from 25 kPa down to about 1-2 kPa; during the same time window the differential pressure on the descending side drops by only about 2 kPa – from 8 kPa down to 6 kPa. For the SB-CL-18 test this is evident from the loop seal differential pressure measurements shown in both Figure 21.4-3 and Figure 21.4-4 of [1]; note that Figure 18.2.1-1a in fact shows the DPE210-LSB and DPE220-LSB measurements for that test shown in Figure 21.4-4.

Similar observation can be made for the 5% break test SB-CL-05, based on the measured loop seal differential pressures shown in Figures 21.5-10 and 21.5-11.

The JAERI-M 62-399 test report for the 2.5% cold leg side break test SB-CL-01 shows that only the broken loop cleared completely; the differential pressures measured in the loop that cleared indicate a dynamics of the loop seal clearance similar to that observed at the 5% break tests SB-CL-05 and SB-CL-18, see Figure RAI.77-1.

Conclusion:

In the updated topical report, the text quoted by NRC in RAI #77, will be modified to state that "*the remaining liquid retained in the cross-over leg after the onset of the loop seal clearing tends to collect in the uphill bend and RCP suction leg*". The updates will be applied in Section 18.2.1 and bullet 7 of Section 18.4.

References:

1. WCAP-16996-P, "Realistic LOCA Evaluation Methodology Applied to the Full Spectrum of Break Sizes (FULL SPECTRUM LOCA Methodology)," November 2010.
2. JAERI-M 89-027,"ROSA-IV/LSTF 5% Cold Leg Break LOCA Experiment Run SB-CL-18 Data Report," March 1989.
3. JAERI-memo 62-399,"ROSA-IV/LSTF 2.5% Cold Leg Break LOCA Experiment Data Report for Runs SB-CL-01, 02 and 03," November 1987.

[ ] a,c

Figure RAI.77-1 – Loop Seal Differential Pressures in the Broken Loop B at ROSA-IV 2.5% Cold Leg Break Test SB-CL-01

Note: This figure is digitized from the respective differential pressure plots shown in Fig.8.13 of the SB-CL-01 dataset in JAERI-M 62-399. Measurement uncertainty is ±0.32kPa.

Question #78: Loop Seal Clearance in LSTF Test SB-CL-14 and Test SB-CL-18

In addition to LSTF Test SB-CL-18, WCAP-16996-P/WCAP-16996-NP, Volumes I, II and III, Revision 0, Section 18, "Loop Seal Clearance," Subsection 18.2.1, "ROSA," presents data from LSTF Test SB-CL-14. Test SB-CL-14 simulated a 10 percent cold leg break, which corresponds to a break area of 0.413 ft^2 or an 8.7 inch equivalent break diameter based on the reference PWR cold leg diameter (27.5 in). Data from 6 ROSA-IV LSTF experiments, Test SB-CL-01, Test SB-CL-05, Test SB-CL-14, Test SB-CL-15, Test SB-CL-16, and Test SB-CL-18, were used for comparison with test predictions obtained with the NRC code TRACE as documented in "TRACE V5.0 Assessment Manual Appendix C: Integral Effects Tests," Agencywide Documents Accession and Management System (ADAMS) No. ML120060172. As indicated by the loop seal differential pressure measurements provided for Test SB-CL-14 in Subsection C.5.5.3, "Simulation of SB-CL-14," in this document, both loop seals experienced clearing between approximately 76 s and 100 s after the break opening. The core uncovered temporarily between approximately 60 s and 80 s just before loop seals clearing and the maximum observed heater rod temperature was about 72 °F (40 K) higher than the initial rod temperature.

WCAP-16996-P/WCAP-16996-NP, Volumes I, II and III, Revision 0, Subsection 18.2.1, "ROSA," includes a single plot of data from Test SB-CL-14, which is shown in Figure 18.2.1-1b, "Measured Pressure Drop in Broken Loop of ROSA 10 percent Break (Koizumi and Tasaka, 1988)." Figure 18.2.1-1b reproduces Figure 6.8, "Loop-B Crossover Leg Differential Pressures," from Reference 3 listed in Subsection 18.5, "References," as: Koizumi, and Tasaka, K., 1988, "Quick Look Report for ROSA-IV/ LSTF 10 percent Cold Leg Break LOCA Test, SB-CL-14," JAERI-memo 63-262. The curves in Figure 18.2.1-1b are marked with symbols labeled as "DP 41" and "DP 42" at the top of the plot. The vertical axis in the plot depicts differential pressure in units of kPa and has a label "DPE210-LSB." Referring to Figure 18.2.1-1b, Subsection 18.2.1 makes the observation that "the liquid tends to be pushed towards the uphill bend and up the pump suction leg" and continues stating that "this suggests that the remaining liquid after loop seal clearing will tend to be collected in the uphill side of the loop seal."

(1) Figure 18.2.1-1b, "Measured Pressure Drop in Broken Loop of ROSA 10 percent Break (Koizumi and Tasaka, 1988)," in WCAP-16996-P/WCAP-16996-NP, Volumes I, II and III, Revision 0, Subsection 18.2.1 shows a reproduction of Figure 6.8 in JAERI-memo 63-262. The graph shown in Figure 18.2.1-1b is not entirely legible. Please provide a legible plot for the data presented in Figure 18.2.1-1b. Explain the availability of Reference 3 in Subsection 18.5 and clarify if electronically recorded data measurements were also available and used as part of the assessment process.

(2) It appears that after the initial transitory period, one of the curves in Figure 18.2.1-1b shows practically zero differential pressure whereas the second one exhibits a rather high and persisting pressure difference, which slowly increases to reach about 30 kPa at the end of the displayed time interval. Some of the measurements from Test SB-CL-14 in Figure 18.2.1-1b are different, both in trend and in magnitude, when compared to the differential pressure measurements shown in Figure 18.2.1-1a, "Measured Pressure Drop in Broken Loop of ROSA 5 percent Break (Kumamaru, et al., 1989)," for Test SB-CL-18. Please explain the basis for asserting in Subsection 18.2.1, "ROSA," that data from both Test SB-CL-18 and Test SB-CL-14, as depicted in Figures 18.2.1-1a and 18.2.1-1b, respectively, support the interpretation that liquid remaining in the loop seal piping following the loop seal clearance "will tend to be collected in the uphill side of the loop seal," when there are obvious and significant disparities between the experimental responses shown in these two figures.

Response:

Reference 3 in Section 18.5, JAERI-memo 63-262, is available to Westinghouse in hardcopy format without electronic data. For this reason, Fig. 6.8 from JAERI-memo 63-262 was copied and presented as Figure 18.2.1-1b in Section 18.2 of the topical report.

As observed by NRC, there is disparity between the measured loop seal differential pressures shown in JAERI-memo 63-262 (Fig. 6.7 and 6.8 therein) and those shown in the TRACE assessment in NRC Publication No. ML120060172 (Figures C.5-122 to C.5-125 therein).

Westinghouse is not aware of the origin and form of the SB-CL-14 test data used in the TRACE assessment (ML120060172). The observed disparity in the loop seal differential pressure measurements in SB-CL-14 is most likely due to inaccurate graphical presentation of the DPE070-LSA and DPE210-LSB measurements in Fig. 6.7 and 6.8 of JAERI-memo 63-262. Note that, as described in its title, JAERI-memo 63-262 is a quick look report and the qualification of the plots, Fig.6.7 and 6.8 in particular, might not have been appropriate. For the DP 17 (DPE070-LSA) and DP 41 (DPE210-LSB) measurements shown in these two plots there must have been a zero-level shift which is estimated to be approximately 30 kPa, so that at about 340 sec the DPE070 and DPE210 measurements trend to <1 kPa.

The following Figures RAI.78-1 and RAI.78-2 show the loop seal differential pressures, obtained by digitizing the curves from Fig. 6.7 and 6.8 of JAERI-memo 63-262 and adjusting the DPE070-LSA and DPE210-LSB plots for the estimated 30 kPa zero-level shift. As seen, with the adjustment, the loop seal differential pressure curves are similar to those shown in Figures C.5-122 to C.5-125 of Appendix C to ML120060172.

Conclusion:

From 80 seconds to 90 seconds liquid holdup in the suction side of the cross-over leg is apparent and the dynamics of the loop seal clearance appears to be similar to that observed at the SB-CL-18 test (see response to RAI 77, Set 6).

Measured collapsed liquid levels in the ROSA 10% cold leg break test SB-CL-09, Fig.4-7 and Fig.4-23 of JAEA-Research 2008-087 [3] show similar loop seal clearance dynamics as well; for convenience copies of these two figures are provided here as Figures RAI.78-3 and RAI.78-4. Therefore, the interpretation that liquid remaining in the loop seal piping following the loop seal clearance will tend to be collected in the uphill side of the loop seal is considered valid. This interpretation is also supported by the full-scale IVO U-Tube test data, briefly discussed in Subsection 18.2.2.4 of [1].

As a result of this response, Figure 18.2.1-1b of the topical report [1] will be replaced with Figure RAI.78-2, presented herein. No other modification in Subsection 18.2.1 is needed as a result of this RAI response.

References:

1. WCAP-16996-P, "Realistic LOCA Evaluation Methodology Applied to the Full Spectrum of Break Sizes (FULL SPECTRUM LOCA Methodology)," November 2010.
2. JAERI-memo 63-262, "Quick Look Report for ROSA-IV/LSTF 10% Cold Leg Break LOCA Test, SB-CL-14," July 1988.
3. JAEA Research 2008-087,"A Study on Rosa/LSTF SB-CL-09 Test Simulating PWR 10% Cold Leg Break LOCA – Loop-seal Clearing and 3D Core Heat-up Phenomena," Japan Atomic Energy Agency, October 2008.

a,c

Figure RAI.78-1 – SB-CL-14 Loop Seal A Differential Pressures

a,c

Figure RAI.78-2 - SB-CL-14 Loop Seal B Differential Pressures

(Measurement uncertainty for DPE070-LSA and DPE210-LSB is ±0.512 kPa, and for DPE080-LSA and DPE220-LSB it is ±0.32 kPa.)

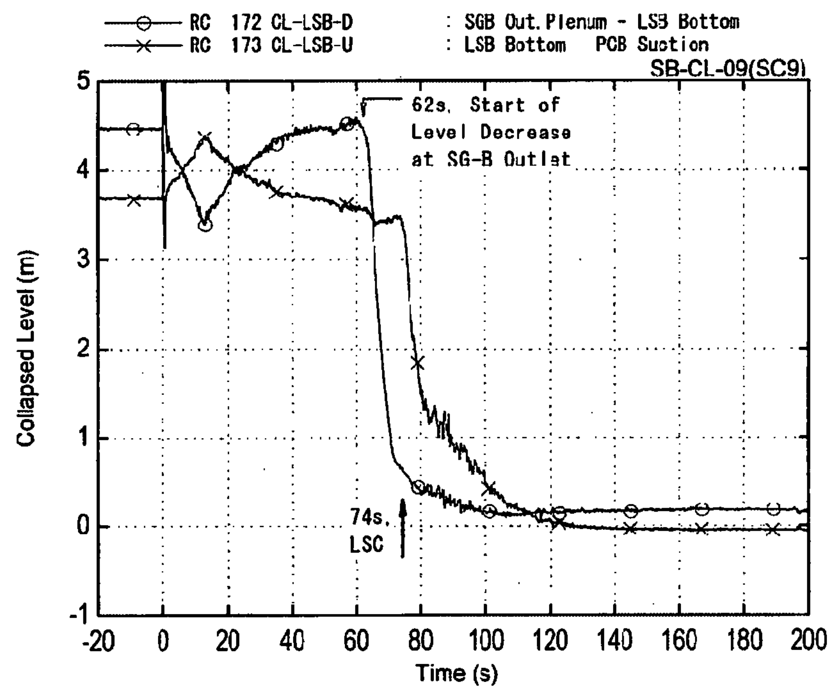

Fig.4-7 Collapsed liquid levels at upflow and downflow sides of Loop-seal B

Figure RAI.78-3 – Copied from JAEA-Research 2008-087 [3]

(Measurement uncertainties are ±0.207 m for CL-LSB-D and ±0.188 m for CL-LSB-U)

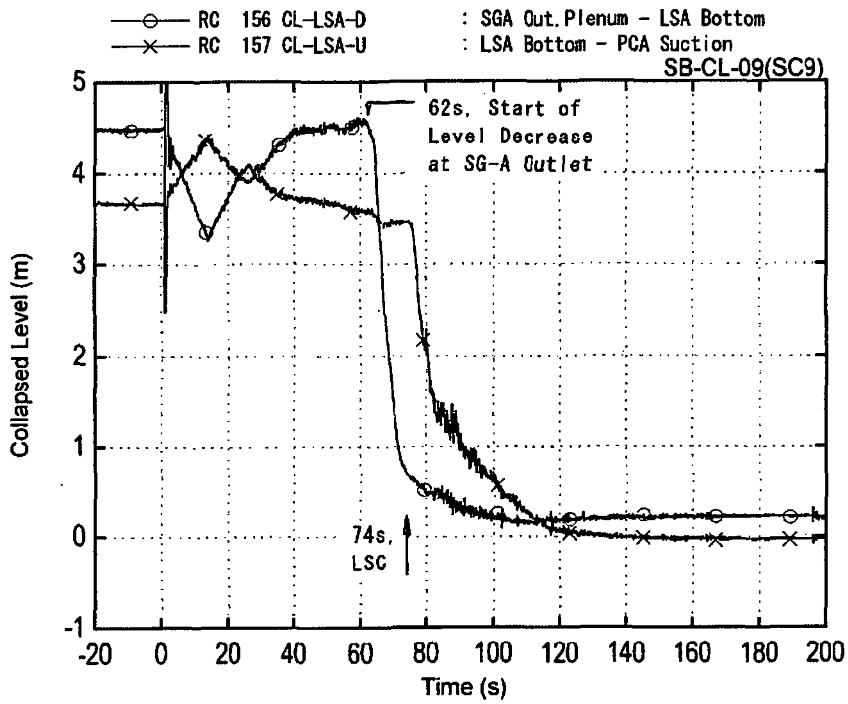

Fig. 4-23 Collapsed liquid levels at upflow and downflow sides of Loop-seal A

Figure RAI.78-4 – Copied from JAEA-Research 2008-087 [3]

(Measurement uncertainties are ±0.207 m for CL-LSA-D and ±0.188 m for CL-LSA-U)

Question #79: WCOBRA/TRAC-TF2 Assessment for LSTF Test SB-CL-14

WCAP-16996-P/WCAP-16996-NP, Volumes I, II and III, Revision 0, Section 18, "Loop Seal Clearance," Subsection 18.2.1, "ROSA," refers to experimental observations from LSTF Test SB-CL-18 and Test SB-CL-14 when discussing loop seal clearance. Subsection 18.4, "Conclusions," states that "assessment of WCOBRA/TRAC-TF2 relative to the experiments indicates" that, among other findings, "the remaining liquid retained after loop seal clearing tends to collect in the uphill bend and RCP suction leg, as demonstrated in the ROSA tests (Section 21)."

WCAP-16996-P/WCAP-16996-NP, Volumes I, II, and III, Revision 0, Section 21, "ROSA-IV Test Simulations," Subsection 21.6.2, "Results and Conclusions for the SB-CL-14 Simulation," presents comparisons of WCOBRA/TRAC-TF2 predictions against Test SB-CL-14 data in Figures 21.6-1 through 21.6-16. Each of Figures 21.6-1 through 21.6-14 and Figure 21.6-16 contain two parts: Part (a), "Code Calculation," and Part (b), "Reported in JAERI-memo 63-262." The graphs included in Part (a) in these figures show code predictions whereas the graphs in Part (b) reproduce data plots from JAERI-memo 63-262. Reference 3 in Subsection 18.5, "References," lists JAERI-memo 63-262 as: Koizumi, and Tasaka, K., 1988, "Quick Look Report for ROSA-IV/LSTF 10% Cold Leg Break LOCA Test, SB-CL-14," JAERI-memo 63-262. Reference 6 in Subsection 21.20, "References," lists the same document as: Koizumi, Y. and Tasaka, K., 1988, "Quick Look Report for ROSA-IV/LSTF 10 percent Cold Leg Break LOCA Test, SB-CL-14," JAERI-memo 63-262. Table 21.1-1, "Selected ROSA-IV Test Series Description and Related Technical Reports," refers to "JAERI-memo 63-262 ('88, Koizumi)."

(1) The excerpts from JAERI-memo 63-262 showing individual graphs in Part (b) in each of Figures 21.6-1 through 21.6-14 and in Figure 21.6-16, are not entirely legible. In addition, the horizontal and vertical axes in these reproduced plots use ranges and scales that are different from the corresponding ones used in the plots showing the code predictions in Part (a) of the assessment figures in Subsection 21.6.2. Some of these figures show only a single calculated parameter in Part (a) and several measured quantities in Part (b), making it unclear which measured quantity, if any, can be used as a legitimate reference parameter for code comparison assessments. Such an approach to analyzing code performance and assessing it against test data does not allow for proper examination of code predictions and their comparison and validation against experimental measurements. Even when a plot compares a single predicted variable against a single measured quantity, comparison is not always straightforward. Often, it is necessary to consider if the model supports a direct comparison between computational results and data. For example, adequate capturing of experimental measuring points and other relevant conditions can require specific nodalization. Please explain and justify the adequacy of the used approach to assessing WCOBRA/TRAC-TF2 best-estimate capabilities as exemplified by the identified assessment analyses presented in WCAP-16996-P/WCAP-16996-NP, Volumes I, II and III, Revision 0, Subsection 21.6, "Simulation of the 10 percent Side Break Test SB-CL-14."

(2) WCAP-16996-P/WCAP-16996-NP, Volumes I, II and III, Revision 0, Subsection 21.6.2, "Results and Conclusions for the SB-CL-14 Simulation," Figure 21.6-7, "Comparison of Loop-B Cross-Over Leg Differential Pressures," Part (a), "Code Calculation," shows predictions for differential pressures in the downhill and uphill sections of the cold leg seal in the broken loop. The calculations presented in Figure 21.6-7 Part (a) appear remarkably different from the test data shown in Figure 21.6-7 Part (b), "Reported in JAERI-memo 63-2." This disparity between code results and test data was not acknowledged in WCAP-16996-P/WCAP-16996-NP, Volumes I, II, and III, Revision 0 Subsection 21.6, "Simulation of the 10 percent Side Break Test SB-CL-14." Please explain why such a pronounced discrepancy in describing an important phenomenon such

as the loop seal clearance remained unidentified and unexplained as part of the WCOBRA/TRAC-TF2 assessment analyses presented in Subsection 21.6.

(3) The WCOBRA/TRAC-TF2 code qualification and assessment of its capabilities of capturing adequately important physical processes and predicting in a best-estimate manner associated governing parameters is found complicated by aspects of the assessment approach as those discussed in Items (1) and (2) above. Based on the resolution of these items, please describe modifications to specific aspects of the WCOBRA/TRAC-TF2 assessment approach in WCAP-16996-P/WCAP-16996-NP, Volumes I, II, and III, Revision 0, if such have been found appropriate for improving the clarity in demonstrating the technical basis for WCOBRA/TRAC-TF2 validation through proper presentation and documentation of results and findings from specific assessment studies. Include results and summarize outcomes from such modifications and revisions of the TR WCAP-16996-P/WCAP-16996-NP, Volumes I, II, and III, Revision 0, as appropriate.

Response:

The comparison plots for the 10% cold leg break test SB-CL-14 (Figures 21.6-1 through 21.6-16 in Section 21 of WCAP-16966-P) have been recreated to compare the code calculations and the test measurements in a single figure. The new set of plots is attached hereafter.

The comparisons of the code calculations against the test data do not change the essence of the discussion and the conclusions in Section 21.6.2 of the Topical Report [1]. However, for consistency with the new set of figures presented herein, the discussion in Section 21.6.2 of [1] is rewritten as follows.

21.6.2 Results and Conclusions for the SB-CL-14 Simulation

Table 21.6-3 summarizes the predicted and measured chronology of events for the 10-percent cold leg test.

Figures 21.6-1 and 21.6-2 show a comparison of the modeled vs. measured pump speed for the two pumps. [

]^{a,c} Beyond 80 seconds the loop flow measurements FE020A/B-LSA and FE160A/B-LSB are unreliable since the flow is two-phase.

The break flow comparison is shown in Figure 21.6-5; the figure presents the test break flow as calculated from the measured level in the catch tank. [

]^{a,c}

[

]^{a,c}

[

]^{a,c}

a,c

Figure RAI.79-1 – Loop-A Pump Speed Comparison
(Measurement uncertainty is 0 Hz)

(New Figure 21.6-1 for WCAP-16996-P)

a,c

Figure RAI.79-2 Loop-B Pump Speed Comparison
(Measurement uncertainty is 0 Hz)

(New Figure 21.6-2 for WCAP-16996-P)

a,c

Figure RAI.79-3 Loop-A Flow Rate Comparison

(Measurement uncertainty is ±1.0008 kg/sec.)

(New Figure 21.6-3 for WCAP-16996-P)

Note: Beyond 80 seconds the loop flow measurements FE020A/B-LSA are unreliable since the flow is two-phase.

a,c

Figure RAI.79-4 Loop-B Flow Rate Comparison
(Measurement uncertainty is ±1.0008 kg/sec.)

(New Figure 21.6-4 for WCAP-16996-P)

Note: Beyond 80 seconds the loop flow measurements FE160A/B-LSA are unreliable since the flow is two-phase.

a,c

Figure RAI.79-5 Comparison of Break Flows

(Measurement uncertainty for the break flow based on catch tank level is not available)

(New Figure 21.6-5 for WCAP-16996-P)

a,c

Figure RAI.79-6 Comparison of Fluid Density in the Break Spool
(Measurement uncertainty is not available)

(New Figure 21.6-6 for WCAP-16996-P)

a,c

Figure RAI.79-7(a) Comparison of Loop-A Cross-Over Leg Differential Pressures
(Measurement uncertainty for DPE070-LSA is ±0.512 kPa, and for DPE080-LSA it is ±0.32 kPa)

(New Figure 21.6-7(a) for WCAP-16996-P)

a,c

Figure RAI.79-7(b) Comparison of Loop-B Cross-Over Leg Differential Pressures
(Measurement uncertainty for DPE210-LSB is ±0.512 kPa, and for DPE220-LSB it is ±0.32 kPa

(New Figure 21.6-7(b) for WCAP-16996-P)

a,c

Figure RAI.79-8 Comparison of System Pressures (Pressurizer and Steam Generator Secondary)
(Measurement uncertainty for PE300-PR is ±0.064 MPa and for PE430-SGA it is ±0.032 MPa)

(New Figure 21.6-8 for WCAP-16996-P)

a,c

Figure RAI.79-9 Comparison of Steam Generator A (SGA) U-tube Inlet-to-top Differential Pressures

(Measurement uncertainty is ±0.064 kPa)

(New Figure 21.6-9 for WCAP-16996-P)

a,c

Figure RAI.79-10 Comparison of Steam Generator B (SGB) U-tube Inlet-to-top Differential Pressures

(Measurement uncertainty is ±0.064 kPa)

(New Figure 21.6-10 for WCAP-16996-P)

a,c

Figure RAI.79-11 Comparison of Steam Generator A (SGA) U-tube Outlet-to-top Differential Pressures

(Measurement uncertainty is ±0.064 kPa)

(New Figure 21.6-11 for WCAP-16996-P)

a,c

Figure RAI.79-12 Comparison of Steam Generator B (SGB) U-tube Outlet-to-top Differential Pressures

(Measurement uncertainty is ±0.064 kPa)

(New Figure 21.6-12 for WCAP-16996-P)

a,c

Figure RAI.79-13(a) Comparison of Steam Generator A (SGA) Inlet Plenum Differential Pressures
(Measurement uncertainty is ±0.256 kPa)

(New Figure 21.6-13(a) for WCAP-16996-P)

a,c

Figure RAI.79-13(b) Comparison of Steam Generator B (SGB) Inlet Plenum Differential Pressures
(Measurement uncertainty is ±0.256 kPa)

(New Figure 21.6-13(b) for WCAP-16996-P)

a,c

Figure RAI.79-14 Comparison of Core Collapsed Liquid Levels
(Measurement uncertainty is not available)

(New Figure 21.6-14 for WCAP-16996-P)

a,c

Figure RAI.79-15(a) Calculated Accumulator A Injection Flow

(New Figure 21.6-15(a) for WCAP-16996-P)

a,c

Figure RAI.79-15(b) Calculated Accumulator B Injection Flow

(New Figure 21.6-15(b) for WCAP-16996-P)

a,c

Figure RAI.79-16 Comparison of High-Power Rod Cladding Temperatures at 6-ft (1830 mm) Core Axial Location

(Measurement uncertainty is ±6.444K)

(New Figure 21.6-16 of WCAP-16996-P)

Question #80: LSTF Test SB-CL-14 Data Qualification

WCAP-16996-P/WCAP-16996-NP, Volumes I, I,I and III, Revision 0, Section 18, "Loop Seal Clearance," Subsection 18.2.1, "ROSA," includes Figure 18.2.1-1b, "Measured Pressure Drop in Broken Loop of ROSA 10 percent Break (Koizumi and Tasaka, 1988)," which reproduces Figure 6.8, "Loop-B Crossover Leg Differential Pressures," from JAERI-memo 63-262. Section 21, "ROSA-IV Test Simulations," Subsection 21.6.2, "Results and Conclusions for the SB-CL-14 Simulation," includes Figure 21.6-7, "Comparison of Loop-B Cross-Over Leg Differential Pressures." Figure 21.6-7 Part (b), "Reported in JAERI-memo 63-262," reproduces the same Figure 6.8, "Loop-B Crossover Leg Differential Pressures," from JAERI-memo 63-262.

Subsection C.5.5.3, "Simulation of SB-CL-14," in "TRACE V5.0 Assessment Manual Appendix C: Integral Effects Tests," ADAMS Accession No. ML120060172, includes Figure C.5-124, "Differential Pressure along downhill Side of Loop-B Seal," and Figure C.5-125, "Differential Pressure along uphill Side of Loop-B Seal." The figures depict DPE210-LSB and DPE220-LSB data signals, respectively, for Test SB-CL-14.

(1) There are apparent and significant disparities between parameters shown in Figure 18.2.1-1b in WCAP-16996-P/WCAP-16996-NP, Volumes I, II and III, Revision 0, Subsection 18.2.1, "ROSA," and in Figures C.5-124 and C.5-125 in "TRACE V5.0 Assessment Manual Appendix C: Integral Effects Tests." In addition, the WCOBRA/TRAC-TF2 calculations in Figure 21.6-7 Part (a), "Code Calculation," differ significantly from the test data in Figure 21.6-7 Part (b), "Reported in JAERI-memo 63-2," which are identical with the test data shown in Figure 18.2.1-1b. Please explain how Test SB-CL-14 measurements presented in Figure 18.2.1-1b, "Measured Pressure Drop in Broken Loop of ROSA 10 percent Break (Koizumi and Tasaka, 1988)," relate to the test data shown in Figures C.5-124, "Differential Pressure along downhill Side of Loop-B Seal," and in Figure C.5-125, "Differential Pressure along uphill Side of Loop-B Seal," in Appendix C, "Integral Effects Tests," of "TRACE V5.0 Assessment Manual."

(2) Please describe test facility selection and test data qualification processes with regard to test data used in WCOBRA/TRAC-TF2 assessment studies if such processes have been considered and applied as part of the WCOBRA/TRAC-TF2 assessment approach implemented in WCAP-16996-P/WCAP-16996-NP, Volumes I, II and III, Revision 0. As part of these processes, please explain if availability of published test reports, documenting measured data, and electronic data files containing recorded measurements were considered and examined. When both types of data sources were available, clarify if a cross-check was performed to examine and qualify important measurements that were used to assess WCOBRA/TRAC-TF2.

(3) Please explain reliance on and use of available information quantifying instrumentation accuracy for test data from experiments that have been selected and used in WCOBRA/TRAC-TF2 assessment studies. Please clarify if such considerations have been applied as part of the approach, implemented in WCAP-16996-P/WCAP-16996-NP, Volumes I, II and III, Revision 0, to asses WCOBRA/TRAC-TF2. Please explain how such aspects of the assessment approach relate to the analyses presented in Section 21, "ROSA-IV Test Simulations," Subsection 21.6, "Simulation of the 10 percent Side Break Test SB-CL-14," of WCAP-16996-P/WCAP-16996-NP, Volumes I, II and III, Revision 0, TR as an example.

(4) Based on the resolution of Items (1) through (3) above, please describe modifications to specific aspects of the WCOBRA/TRAC-TF2 assessment approach in WCAP-16996-P/WCAP-16996-NP, Volumes I, II and III, Revision 0, if such have been found appropriate for improving the

clarity in demonstrating the technical basis for WCOBRA/TRAC-TF2 validation through proper, accurate, and adequate presentation and documentation of results and findings from specific assessment studies. Include results and summarize outcomes and revisions of the WCAP-16996-P/WCAP-16996-NP, Volumes I, II and III, Revision 0, TR from such modifications as appropriate.

Response:

Regarding Part (1), see responses to Questions 78 and 79.

Regarding Part (2), Westinghouse has provided a response to NRC Question 76 which uses scaling analysis to highlight the suitability of the ROSA-IV Large Scale Test Facility as the IET of choice for the WCOBRA/TRAC-TF2 code validation.

With regards to the ROSA test data qualification, [

]^{a,c}

Regarding Part (3), each of the JAERI test reports documenting the simulated ROSA-IV tests includes detailed information on the accuracy of the instrument measurements and data qualification. Westinghouse has relied on that information to make engineering judgments with respect to the validity of the test data but has not performed any additional instrument accuracy analysis or assessment beyond that already available in the respective JAERI reports.

Regarding Part (4), the updated topical report will include the revised figures and text, as stated in the responses to questions 77, 78 and 79.

Question #81: ROSA-IV LSTF WCOBRA/TRAC-TF2 Assessment Results Presentation

In RAI questions 78, 79, and 80, additional information was requested to clarify aspects related to both the use of ROSA-IV LSTF test data as well as the presentation and comparison of WCOBRA/TRAC-TF2 predictions against test data in WCAP-16996-P/WCAP-16996-NP, Volumes I, II and III, Revision 0, Section 18, "Loop Seal Clearance," and in Section 21, "ROSA-IV Test Simulations," to demonstrating and assessing the code performance. With regard to the experimental database used in WCAP-16996-P/WCAP-16996-NP, Volumes I, II and III, Revision 0, Section 21, Subsection 21.1, "Introduction," refers to Table 21.1-1, "Selected ROSA-IV Test Series Description and Related Technical Reports," and states: "Table 21.1-1 shows the list of tests used for the validation work. It contains relevant reports and articles related to the ROSA-IV LSTF and the different test considered herein." WCAP-16996-P/WCAP-16996-NP, Volumes I, II and III, Revision 0, Section 21, "ROSA-IV Test Simulations," Subsection 21.5.2, "Results and Conclusions from the SB-CL-05 Simulation," in discussing WCOBRA/TRAC-TF2 assessment results, states: "Unfortunately, the SB-CL-05 electronic data file available in Westinghouse does not contain any recorded fuel rod cladding temperature measurements so that direct graphical comparison cannot be presented. However, rod cladding temperatures measured at the test can be found in Figure 5.468 through Figure 5.484 of the SB-CL-05 test report (Kawaji, et.al.)." Subsection 21.20, "References," identifies only one work by Kawaji listed in Reference 3 as: "Kawaji, M., et al., 1986, "ROSA-IV/LSTF 5 percent Cold Leg Break LOCA Experiment Data Report, Run SB-CL-05," JAERI-memo 61-056."

In addition to addressing RAI questions 78, 79, and 80, the staff finds it necessary to request clarification of the following items.

(1) Please present a table that documents the source and type of experimental data from experiments performed at the ROSA-IV LSTF integral effect test facility and used to assess WCOBRA/TRAC-TF2 for the purpose of the Full Spectrum LOCA Methodology development as presented in WCAP-16996-P/WCAP-16996-NP, Volumes I, II and III, Revision 0. The table should contain the following pieces of information, each presented in a separate column: (1) test run (experiment) identifiers, (2) identification of data channel identifiers (experimental instrument tags) for measurements used to assess WCOBRA/TRAC-TF2, (3) accuracies of the sensors used in each data channel, (4) availability of electronic test data files and if the files contain the identified experimental measurements, (5) test reports documenting the identified experimental measurements, (6) any other sources of information describing the identified experimental measurements, (7) if examination of the identified experimental measurements (data channel signals) was performed to qualify the data as appropriate for code assessment. Please list each separate experiment (test run) separately in the table. If appropriate, please group data channels based on the type of measurements (for example, temperature, differential pressure, etc.) and list the groups in separate rows when providing their characteristics (accuracies, data sources, examination status). Please provide the meaning of the symbols used in the instrument tags (for example, "TE" for fluid temperature, "DP" for differential pressure, "TW" for wall temperature, etc.).

(2) When plotting WCOBRA/TRAC-TF2 code predictions against ROSA-IV LSTF test measurements that are considered of key importance for assessing the code capabilities, please explain why the depicted code predictions and test data represent a valid comparison for judging the code performance. In particular, it is important that the model nodalization reflects adequately experimental measuring points. For example, the computational node for a temperature prediction should closely match the location of the thermocouple used in the test. Also, when computing differential pressures for comparison against data, nodalization aspects and locations of

differential pressure taps in the experiment should be considered. As appropriate, please include diagrams showing model nodalization and sensor locations in the same figure.

(3) Please redraw the figures that are used in WCAP-16996-P/WCAP-16996-NP, Volumes I, II and III, Revision 0, to compare WCOBRA/TRAC-TF2 prediction results against ROSA-IV LSTF test measurements so that both the data measurements and the code predictions are depicted in a single common graph. Please plot the error bars associated with the presented test data when information is available.

(4) Please revise WCAP-16996-P/WCAP-16996-NP, Volumes I, II and III, Revision 0, to include the additional information requested in Items (1) through (3) above as found appropriate.

Response:

Regarding Parts (1) and (2) of the RAI:
All the requested information is already available in the JAERI reports. The noding of the ROSA test facility is fairly consistent with the location of the various measurement instruments. In the generated comparison plots for the ROSA test simulations, presented in WCAP-16996-P, code calculated pressures were adjusted wherever there was a significant mismatch between the hydraulic node center and the real physical location of the measurements.

Regarding Parts (3) and (4), the updated topical report will include the revised figures and text, as stated in the responses to questions 77, 78 and 79.

Question #82: Break Equivalent Diameter in LSTF Tests SB-CL-01, SB-CL-02, and SB-CL-03

WCAP-16996-P/WCAP-16996-NP, Volumes I, II and III, Revision 0, Section 21, "ROSA-IV Test Simulations," Subsection 21.7.2.1, "2.5 percent Tests," presents WCOBRA/TRAC-TF2 assessment results against three ROSA-IV LSTF tests simulating a 2.5 percent cold leg break with different break orientations. Test SB-CL-01 simulated a side break, Test SB-CL-02 studied a bottom break, and Test SB-CL-03 examined a top break. All three tests used an orifice with a 16.0 mm (0.63 inch) opening diameter to model the break. Assessment results are shown in Subsection 21.7.2.1 Figures 21.7-3 through 21.7-10. Subsection 21.7.2, "Discussion of Results," states that Test SB-CL-01, Test SB-CL-02, and Test SB-CL-01-03 "simulated a 2.5 percent break in the cold leg, which approximates a 3 inch break in a PWR."

The 16.0 mm (0.63 inch) ID orifice, used to simulate a 2.5 percent cold leg break in the identified ROSA-IV LSTF tests, had an opening area of 201.1 mm^2 (0.00216 ft^2). The LSTF reference PWR cold leg ID was 27.5 inch. Based on the LSTF volumetric scaling ratio, the 2.5 percent LSTF break size scales to a corresponding PWR cold leg break area, as follows:

PWR Break Area = 48 × LSTF Break Area = 48 × 0.00216 ft^2 = 0.1037 ft^2.

The above determined 2.5 percent PWR cold leg break area of 0.1037 ft^2 corresponds to an equivalent break diameter of 4.36 inch. This equivalent break diameter significantly differs from the 3 inch equivalent break diameter that is cited in WCAP-16996-P/WCAP-16996-NP, Volumes I, II and III, Revision 0, Subsection 21.7.2, "Discussion of Results." Please explain how it was determined in Subsection 21.7.2, "Discussion of Results," that ROSA-IV LSTF Test SB-CL-01, Test SB-CL-02, and Test SB-CL-01-03 "simulated a 2.5 percent break in the cold leg, which approximates a 3 inch break in a PWR."

Response:

The statement in Section 21.7.2 of the FSLOCA™ Topical Report [1] that the ROSA-IV 2.5-percent break tests SB-CL-01, -02, and -03 approximate a 3-inch break in a PWR is too general and apparently inaccurate if applied specifically to a 4-loop Westinghouse PWR, which is volume-scaled 48:1 relative to the ROSA-IV LSTF. Westinghouse agrees with the NRC's calculation that the ROSA 2.5% break tests represent an equivalent 4.36-inch diameter break of the reference 4-loop Westinghouse PWR.

At the same time, the 2.5% ROSA cold leg break would represent a 3.45-inch break if applied to the 3-loop Beaver Valley Unit 1 (DLW), which is approximately 30:1 volume-scaled relative to ROSA; for a 2-

loop PWR the equivalent break size would be even smaller than the 3.45-inches determined for DLW. The relevant text in Section 21.7.2 of the FSLOCA Topical Report [1] will be modified by removing the 3-inch value provided for the equivalent break size of a PWR. The following text will be provided in Section 21.7.2 of the updated topical report.

In LSTF, the break unit can be configured such that the break orientation effect can be studied. Two sets of three experiments were conducted in the LSTF to investigate the effect of break orientation. The first three tests (SB-CL-01, -02, and -03; side, bottom and top respectively), simulated a 2.5 % break in the cold leg, ~~which approximates a 3 inch break in a PWR~~. The second three tests (SB-CL-12, -15 and -16) simulated a 0.5% break in the cold leg. In this section these two sets of break orientation studies will be discussed.

References

1. WCAP-16996-P, “Realistic LOCA Evaluation Methodology Applied to the Full Spectrum of Break Sizes (FULL SPECTRUM LOCA Methodology),” November 2010.

Question #86: MSTRTX, STRTX, STRTX1, and STRTX2 Multipliers

WCAP-16996-P/WCAP-16996-NP, Volumes I, II, and III, Revision 0, Section 10, "WCOBRA/TRAC-TF2 One-Dimensional Component Models," Subsection 10.2, "Pipe Component," explains that in addition to the HS_SLUG multiplier, "user specified allowances for horizontal stratification within a PIPE component can be provided through the MSTRTX and STRTX input." Subsection 10.3, "TEE Component," states that "similar to the PIPE component, the user has the option to specify allowance for horizontal stratification in the main and side pipes through the STRTX1 and STRTX2 multipliers."

WCAP-16996-P/WCAP-16996-NP, Volumes I, II, and III, Revision 0, provides no description of the MSTRTX, STRTX, STRTX1, and STRTX2 multipliers. At the same time, Figure 21.3-9, "Hot Leg (Including Pressurizer), Steam Generator and Cross-Over Leg Noding," in Section 21, "ROSA-IV Test Simulations," of the WCAP-16996-P/WCAP-16996-NP, Volumes I, II and III, Revision 0, shows that specific values of STRTX linked to the common interface between the two adjacent cells used to model each of the 90° bends connecting the horizontal section of the LSTF loop seal to the downhill and uphill pipes of the cross-over leg.

(1) The MSTRTX, STRTX, STRTX1, and STRTX2 multipliers appear to be related to the modeling of important process in horizontal two-phase flow such as flow stratification. Please explain why the MSTRTX, STRTX, STRTX1, and STRTX2 multipliers were not described in WCAP-16996-P/WCAP-16996-NP, Volumes I, II, and III, Revision 0.

(2) Please explain the meaning of the MSTRTX, STRTX, STRTX1, and STRTX2 multipliers, their modeling impact, and intended use. Provide the definitions of these quantities and describe how they relate to specific WCOBRA/TRAC-TF2 models and expressions.

(3) WCAP-16996-P/WCAP-16996-NP, Volumes I, II and III, Revision 0, Subsection 10.2, "Pipe Component," states that "user specified allowances for horizontal stratification within a PIPE component can be provided through the MSTRTX and STRTX input." Please clarify if MSTRTX, STRTX, STRTX1, and STRTX2 are user defined input parameters. Describe their initialization, default values, and allowable input ranges.

(4) Please explain how the default values and allowable input ranges for MSTRTX, STRTX, STRTX1, and STRTX2 have been determined and present the technical basis for their validation for the purposes of PWR LOCA analyses using WCOBRA/TRAC-TF2. Describe how the values of these multipliers are assigned and controlled in PWR plant LOCA analyses. Please relate the responses to Items (2) and (3) above to specific features of PWR plant models used for LOCA analyses. Identify specific components in such models that are affected by these parameters. Please present diagrams from a reference plant model to explain and illustrate their application in PWR LOCA analyses.

(5) Please revise WCAP-16996-P/WCAP-16996-NP, Volumes I, II, and III, Revision 0, to include the additional information as requested in Items (2) through (4) above.

Response:

(1) The STRTX input flag is important to the modeling of flow stratification in the loop seal region. The description of this input flag is provided in Section 10.2 of WCAP-16696-P [1], and the application of the

input flag is alluded to in Section 29.5.6 of WCAP-16996-P. It is important to clarify that the MSTRTX, STRTX, STRTX1, and STRTX2 input flags are not multipliers, as described in part (2) of this response.

(2) The value of the MSTRTX input flag only determines whether additional inputs are specified for certain components; it does not directly impact the WCOBRA/TRAC-TF2 calculated results. MSTRTX can be input for PIPE and TEE components; the allowable input values are 0 and 1. If MSTRTX = 0 for a given PIPE or TEE component, then the STRTX, STRTX1, and STRTX2 flags are not specified as part of the component input. If MSTRTX = 1, then STRTX, STRTX1, and/or STRTX2 are included as part of the component input.

The STRTX, STRTX1, and STRTX2 input flags are all equivalent (i.e., they all have the same function); the differentiation is only in the component to which they are input. STRTX is input for PIPE components; STRTX1 for the main line of TEE components; and STRTX2 for the branch line of TEE components. [

]a,c

(3) The MSTRTX, STRTX, STRTX1, and STRTX2 input flags are all user defined. The default value of MSTRTX is 0, and by default the STRTX, STRTX1, and STRTX2 parameters are not input. The allowable entries for MSTRTX are 0 and 1, as described in Part (2) of this response. The allowable entries for STRTX, STRTX1, and STRTX2 (when MSTRTX = 1) are 0, 1, and 2: [

]a,c

(4) MSTRTX = 0 (STRTX, STRTX1, and STRTX2 not input) is specified for [

]a,c This modeling approach was selected for consistency with the supporting Separate Effects Test (SET) and Integral Effects Test (IET) simulations. The input values are controlled by code diagnostics and analyst guidance.

(5) The FSLOCA topical report will be updated to reflect the information discussed in this RAI response. The first paragraph in Section 29.5.6 of WCAP-16996-P under the "Horizontal Stratification" heading will be replaced with the following:

> *The prediction of the horizontal stratified flow regime in the loop seal piping was assigned a high (H) ranking in the loop seal clearance period of a small break LOCA. The flow is allowed to stratify at all cell faces in the loop seal region where the inclination angle is [*
>
> *]^{a,c} The uncertainty on the flow regime transition in and out from horizontal stratified (or wavy-dispersed) flow is treated as discussed in Section 29.1.7 (HS_SLUG). [*
>
> *]^{a,c}*

Additionally, the use of the user-specified input flag (STRTX = 1) will be described for all models where it is applied.

Reference(s)

1) WCAP-16996-P, "Realistic LOCA Evaluation Methodology Applied to the Full Spectrum of Break Sizes (FULL SPECTRUM LOCA Methodology)," November 2010.

a,c

Figure 86-1: Illustration of Flow Stratification Checks for a Pressurized Water Reactor Crossover Leg

Question #87: WCOBRA/TRAC-TF2 Non-Sampled Modeling Multipliers

As addressed in RAI question #86, the MSTRTX, STRTX, STRTX1, and STRTX2 multipliers, although related to the modeling of the highly ranked phenomenon of horizontal two-phase flow stratification, were not described in WCAP-16996-P/WCAP-16996-NP, Volumes I, II, and Ill, Revision 0. At the same time, it appears that one such parameter, STRTX, was applied in WCOBRA/TRAC-TF2 assessment studies as indicated in Figure 21.3-9, "Hot Leg (Including Pressurizer), Steam Generator and Cross-Over Leg Noding," in WCAP-16996-P/WCAP-16996-NP, Volumes I, II, and Ill, Revision 0, Section 21, "ROSA-IV Test Simulations."

(1) Please provide a table that lists all parameters and multipliers related to the modeling of physical processes in WCOBRA/TRAC-TF2 and that are available for user input. The table should include separate columns that describe the following types of information: (1) the parameter identifier (for example, STRTX), (2) the PIRT ranking for the process to which the parameter applies, (3) the analytic expression for the relation where the parameter appears as coded in the code source, (4) a summary description of the physical phenomenon to which the parameter applies, and (5) default value and allowable input range for the parameter, as applicable. The parameters listed in the table should include all user defined quantities that are available in addition to the input parameters treated as random variables in the Full Spectrum LOCA methodology and described in WCAP-16996-P/WCAP-16996-NP, Volumes I, II, and Ill, Revision 0, Section 29, "Assessment of Uncertainty Elements."

(2) Please explain how the default values and allowable input ranges for the parameters identified in the response to Item (1) above have been determined and present the technical basis for their validation. Describe how the values of these multipliers are assigned and controlled in PWR plant LOCA analyses using WCOBRA/TRAC-TF2.

Response:

The information requested was largely provided previously in response to Requests for Additional Information (RAIs) 50 and 77 on the FULL SPECTRUM LOCA (FSLOCA) Evaluation Model (EM) per LTR-NRC-13-73 [1]. A comprehensive list of the user-defined multipliers is provided in Table 50-1 of the response to RAI 50. The multipliers sampled in the uncertainty analysis (user-input or generic) are described in Table 50-2. These tables contain the parameter names, descriptions, ranges, default value (for user-input multipliers), and distribution (for sampled multipliers).

The Phenomena Identification and Ranking Table (PIRT) ranking, analytic expression, related physical phenomenon, and other information for the sampled variables are described in Table 1 of the response to RAI 77. There are several user-defined multipliers listed in Table 50-1 of the response to RAI 50 for which this information was not specified. This is generally because either a) the multiplier was part of the base TRAC-P Version 5.4.28 code and is not used within the FSLOCA methodology, or b) the multiplier was introduced during the method development and later determined to be unnecessary and therefore is unused for the FSLOCA methodology. An explanation of such parameters was provided in Table 50-3 of the response to RAI 50.

It is recognized that MSTRTX, STRTX, STRTX1, and STRTX2 do not appear in any of the tables in response to RAIs 50 and 77. These input flags were not included because they are not multipliers, but

rather allow the user to [ ]^{a,c} as described in the response to RAI 86. Generally the application of such input flags is described in WCAP-16996-P [2]; however, in this particular case the topical report description was inadequate, and will be updated as discussed in the response to RAI 86.

There are a few other parameters which were not included in Table 50-2 of the response to RAI 50 since they are not direct multipliers within WCOBRA/TRAC-TF2; but they do modify code inputs. For example, the [ ]^{a,c} which is input into the code. For completeness, the equivalent information for these parameters is provided in Table 87-1.

Table 87-1: Supplement to Table 50-2, Indirect Multipliers Subject to Sampling in the Uncertainty Analysis

Acronym	Identifier	Sampling Range	Distribution	Reference
[				
				]^{a,c}

Reference(s)

1) LTR-NRC-13-73, "Submittal of Westinghouse Responses to 'WCAP-16996-P, 'Realistic LOCA Evaluation Methodology Applied to the Full Spectrum of Break Sizes (FULL SPECTRUM LOCA Methodology)' Request for Additional Information – RAIs 46 – 58, 75 and 77' (Proprietary/Non-Proprietary), Project 700, TAC No. ME5244," October 28, 2013.

2) WCAP-16996-P, "Realistic LOCA Evaluation Methodology Applied to the Full Spectrum of Break Sizes (FULL SPECTRUM LOCA Methodology)," November 2010.

Question #93: Editorial Findings

Please address the findings identified below as they apply to various subsections of Section 21, "ROSA-IV Test Simulations," in Volume 2 of WCAP-16996-P/WCAP-16996-NP, Volumes I, II, and III, Revision 0.

(1) Subsection 21.4.3 states on page 21-8 that "Figures 21.4-1 through 22.4-20 compare predicted and measured results for the 5-percent cold leg break test SB-CL-18." Please explain if Figure 22.4-20 has been referred to in error instead of Figure 21.4-20 on page 21-8 of WCAP-16996-P/WCAP-16996-NP, Volumes I, II, and III, Revision 0, and correct if appropriate.

(2) WCAP-16996-P/WCAP-16996-NP, Volumes I, II, and III, Revision 0, Subsection 21.5.2, "Results and Conclusions from the SB-CL-05 Simulation," refers to Figures 21.6-7(a) and 21.6-7(b) on page 21-12 when discussing SG secondary side pressure in each loop. Please explain if Figures 21.6-7(a) and 21.6-7(b) have been referred to in error instead of Figures 21.5-7(a) and 21.5-7(b) on page 21-12 of WCAP-16996-P/WCAP-16996-NP, Volumes I, II, and III, Revision 0, and correct if appropriate.

(3) WCAP-16996-P/WCAP-16996-NP, Volumes I, II, and III, Revision 0, Subsection 21.16.2 is entitled "HS_SLUG Sensitivity with 5 percent Top Break test SB-CL-18." The first sentence in this subsection reads: "Two simulations of the 5 percent side break test SB-CL-18 test were performed with setting the HS_SLUG multiplier at its maximum [ ]^{a,c} and minimum [ ]^{a,c} values." Please confirm the LSTF test run that is considered in Subsection 21.16.2, verify the break orientation angle for this test, and provide relevant corrections if appropriate. Please check the proper wording of the sentence cited above.

(4) WCAP-16996-P/WCAP-16996-NP, Volumes I, II, and III, Revision 0, Section 21, "ROSA-IV Test Simulations," Subsection 21.11.2, "SB-CL-18 Simulation Without Hot Leg Nozzle Bypass Flow," states on page 21-33: "The results of this sensitivity, taken in conjunction with these presented in the previous Section 21.11.2, also shows that modeling lower overall bypass is conservative." Please confirm the subsection number referred to in this citation from Subsection 21.11.2 and correct the wording of the sentence as appropriate.

Response:

(1) WCAP-16996-P/WCAP-16996-NP, Volume II, Revision 0, Subsection 21.4.3, paragraph five, first sentence will be corrected to read "Figures 21.4-1 through 21.4-20 compare predicted and measured results for the 5-percent cold leg break test SB-CL-18.".

(2) WCAP-16996-P/WCAP-16996-NP, Volume II, Revision 0, Subsection 21.5.2, paragraph eight, first and second sentences will be corrected to read [ ]^{a,c}

[

]a,c.

(3) WCAP-16996-P/WCAP-16996-NP, Volume II, Revision 0, Subsection 21.16.2, the title will be corrected to read "HS_Slug Sensitivity with 5% Side Break test SB-CL-18".

(4) WCAP-16996-P/WCAP-16996-NP, Volume II, Revision 0, Subsection 21.11.2, paragraph four, last sentence will be corrected to read **[**

]a,c

RAI Question #112: Sensitivity of WCOBRA/TRAC-TF2 Small Break LOCA Predictions to Steam Generator Nodalization

Please present sensitivity results for a reference four-loop Westinghouse plant using WCOBRA/TRAC-TF2, which examine the effect of SG nodalization on small break LOCA predication results. Show the sensitivity impact for the limiting small break size, which yields the most severe core level suppression for the selected PWR plant model and applying nominal input parameters.

(1) Please present code results using a standard SG nodalization scheme, adopted for WCOBRA/TRAC-TF2 modeling of SGs with inverted U-tubes, and a refined noding in which the number of nodes representing the SG U-tube bundle is doubled. In particular, explain and present sensitivities to refined nodalization of the 180°-bend region of the U-tube bundle.

(2) Please present sensitivity results as requested in Item (1) above when the SG U-tube bundle in each PWR primary loop is modeled using two and tree pipe hydraulic components. In modeling the U-tubes in each SG bundle by multiple pipe components, please split the U-tubes into individual groups based on the U-tube apex elevations so that the tallest, middle, and shortest tubes are represented by individual hydraulic components.

(3) In responding to Items (1) and (2) above, please include, among others, comparison plots for the SG U-tube upside and downside collapsed liquid levels in the broken and intact loops, uphill and downhill loop seal collapsed liquid levels in the broken and intact loops, vessel core-side and downcomer-side collapsed liquid levels, core void fractions, and peak clad temperatures.

Response:

The steam generator (SG) model used in the pressurized water reactor (PWR) examples in the FULL SPECTRUM™ LOCA (FSLOCA™) Topical Report [1] is based on a combination of PIPE, TEE, and HTSTR components. A single PIPE component is used to model the entire primary side U-tube bundle. The primary-to-secondary heat transfer is modeled by using a HTSTR component that connects the primary side PIPE and the secondary side, which is modeled by a TEE component. This steam generator model has been validated against test data from the ROSA-IV Large Scale Test Facility (LSTF) as shown in Section 21 of the topical report [1].

In this response, sensitivity studies have been performed to assess the impact of different steam generator nodalization to the PWR SBLOCA transient. The base case of this study is the most conservative [ ]^{a,c} SBLOCA case from Beaver Valley Unit 1, which is the reference 3-loop Westinghouse PWR for the SBLOCA parametric study to support an NRC audit on FSLOCA [2]. The postulated split break occurs in the cold leg of loop 1 with the break size of [ ]^{a,c}. With the most conservative parameters combined in the base run, severe core level suppression occurred and the PCT reached [ ]^{a,c}. There are two sensitivity studies performed per the RAI. The first sensitivity study is to refine the noding in the steam generator tubes and the second one utilizes three parallel PIPE components instead of one PIPE to model the steam generator tubes. The results of the studies will be presented followed by conclusive remarks.

Sensitivity Study 1: Double the Nodes in the Steam Generator Tubes

In the first sensitivity study, the node size of the vertical tubes (both uphill and downhill) is reduced to a half of the original node size in the base run as shown in Figure 112-1. In the base run, [

]^{a,c}

To demonstrate the water distribution in the steam generators and loop seals in the SBLOCA transient, in lieu of collapsed liquid level, an equivalent average void fraction is used in the steam generator and loop seal plots of the two sensitivity studies. Low void fraction indicates high collapsed liquid level while high void fraction means less water in the component. The results of this sensitivity study are presented in Figures 112-2 through 112-17. Figures 112-2, 112-3 and 112-4 show the average void fraction at the uphill side of U-tubes in the respective steam generator 1, steam generator 2, and steam generator 3. The SG noding difference only creates [

]^{a,c}

Sensitivity Study 2: Three Parallel PIPEs Modeling the Steam Generator Tubes

In the base run, the SG U-tubes are modeled with one PIPE component. In this noding sensitivity study, the U-tube PIPE component is replaced by three parallel PIPE components. The three parallel PIPEs are merged to the steam generator inlet and outlet plenums similar to the physical layout of the steam generator as shown in Figure 112-18. [

]^{a,c}

The results of this sensitivity study are presented in Figures 112-19 through 112-34. Similar to the first sensitivity study, average void fraction is used to demonstrate the water distribution in the steam generators and loop seals. Figures 112-19, 112-20 and 112-21 show the average void fraction at the uphill side of U-

tubes in the respective steam generator 1, steam generator 2, and steam generator 3. [

]a,c

Conclusive Remarks

The sensitivity studies on the steam generator nodalization indicate that in general the SBLOCA transient is not sensitive to the noding changes studied herein. [

]a,c

References:

1. WCAP-16996-P, "Realistic LOCA Evaluation Methodology Applied to the Full Spectrum of Break Sizes (FULL SPECTRUM™ LOCA Methodology)," November 2010.
2. LTR-NRC-13-70, "Summary of July 2013 NRC Code Workshop and August 2013 NRC Audit of the FULL SPECTRUM LOCA (FSLOCA) Evaluation Model (Proprietary/Non-Proprietary)," October 2013.
3. LTR-NRC-13-73, "Submittal of Westinghouse Responses to WCAP-16996-P, "Realistic LOCA Evaluation Methodology Applied to the Full Spectrum of Break Sizes (FULL SPECTRUM LOCA Methodology' Requests for Additional Information – RAIs 46 – 58, 75 and 77," (Proprietary)," November 2013.

a,c

Figure 112-1. Comparison of SG nodalization in the base run (left) and the revised one with doubled SG tube nodes (right). (Sensitivity Study 1)

a,c

Figure 112-2. Comparison of SG 1 U-tube uphill average void fraction. (Sensitivity Study 1)

a,c

Figure 112-3. Comparison of SG 2 U-tube uphill average void fraction. (Sensitivity Study 1)

a,c

Figure 112-4. Comparison of SG 3 U-tube uphill average void fraction. (Sensitivity Study 1)

a,c

Figure 112-5. Comparison of SG 1 U-tube downhill average void fraction. (Sensitivity Study 1)

a,c

Figure 112-6. Comparison of SG 2 U-tube downhill average void fraction. (Sensitivity Study 1)

a,c

Figure 112-7. Comparison of SG 3 U-tube downhill average void fraction. (Sensitivity Study 1)

a,c

Figure 112-8. Comparison of loop seal 1 downhill average void fraction. (Sensitivity Study 1)

a,c

Figure 112-9. Comparison of loop seal 2 downhill average void fraction. (Sensitivity Study 1)

a,c

Figure 112-10. Comparison of loop seal 3 downhill average void fraction. (Sensitivity Study 1)

a,c

Figure 112-11. Comparison of loop seal 1 uphill average void fraction. (Sensitivity Study 1)

a,c

Figure 112-12. Comparison of loop seal 2 uphill average void fraction. (Sensitivity Study 1)

a,c

Figure 112-13. Comparison of loop seal 3 uphill average void fraction. (Sensitivity Study 1)

a,c

Figure 112-14. Comparison of core collapsed liquid level. (Sensitivity Study 1)

a,c

Figure 112-15. Comparison of core void fraction. (Sensitivity Study 1)

a,c

Figure 112-16. Comparison of downcomer collapsed liquid level. (Sensitivity Study 1)

a,c

Figure 112-17. Comparison of PCT. (Sensitivity Study 1)

a,c

Figure 112-18. Comparison of SG nodalization in the base input (left) and the revised one with three steam generator tube components (right). (Sensitivity Study 2)

a,c

Figure 112-19. Comparison of SG 1 U-tube uphill average void fraction. (Sensitivity Study 2)

a,c

Figure 112-20. Comparison of SG 2 U-tube uphill average void fraction. (Sensitivity Study 2)

a,c

Figure 112-21. Comparison of SG 3 U-tube uphill average void fraction. (Sensitivity Study 2)

a,c

Figure 112-22. Comparison of SG 1 U-tube downhill average void fraction. (Sensitivity Study 2)

a,c

Figure 112-23. Comparison of SG 2 U-tube downhill average void fraction. (Sensitivity Study 2)

a,c

Figure 112-24. Comparison of SG 3 U-tube downhill average void fraction. (Sensitivity Study 2)

a,c

Figure 112-25. Comparison of loop seal 1 downhill average void fraction. (Sensitivity Study 2)

a,c

Figure 112-26. Comparison of loop seal 2 downhill average void fraction. (Sensitivity Study 2)

a,c

Figure 112-27. Comparison of loop seal 3 downhill average void fraction. (Sensitivity Study 2)

a,c

Figure 112-28. Comparison of loop seal 1 uphill average void fraction. (Sensitivity Study 2)

a,c

Figure 112-29. Comparison of loop seal 2 uphill average void fraction. (Sensitivity Study 2)

a,c

Figure 112-30. Comparison of loop seal 3 uphill average void fraction. (Sensitivity Study 2)

a,c

Figure 112-31. Comparison of core collapsed liquid level. (Sensitivity Study 2)

a,c

Figure 112-32. Comparison of core void fraction. (Sensitivity Study 2)

a,c

Figure 112-33. Comparison of downcomer collapsed liquid level. (Sensitivity Study 2)

a,c

Figure 112-34. Comparison of PCT. (Sensitivity Study 2)